

# Bi-Directional *CLLC* Resonant Converter with Integrated Planar Transformer for Energy Storage Systems

Abhinav Soni<sup>1</sup>, Student, Ajeet K. Dhakar<sup>2</sup>, Member, IEEE  
Central Electronics Engineering Research Institute-CSIR, Pilani, India

**Abstract**—This paper presents a bi-directional *CLLC* resonant converter for Energy storage Systems applications, with an integrated planar transformer to enhance power density and curtail the parasitic elements in the transformer. The passive elements in any converter account for the bulkiness, and it can be vanquished by increasing the switching frequency, which can only be entailed by a planar magnetic structure and wide bandgap devices like gallium nitride (GaN) and silicon carbide (Si). Further, FEA analysis is performed to estimate leakage, AC resistance, and core losses for an integrated planar transformer. A simplified voltage/current loop control is implemented on a 32-bit digital signal processor (TMS320F28379D) for battery charging. The advantage of the proposed transformer design is validated through a 300-350 kHz, 500-750 W *CLLC* resonant converter with a peak efficiency of 96.60%

**Keywords**—Isolated bi-directional converter (IBDC), *CLLC*, Energy storage system (ESS), finite element analysis (FEA), Zero voltage switching (ZVS) and Zero current switching (ZCS)

## I. INTRODUCTION

Energy Storage Systems are gaining momentum to be the future's power system. For the commercial/industrial sector, the energy storage system can help alleviate the effect of the utility grid disturbance and can direct power either from the grid to battery pack during peak-off hours or from the battery pack to the grid during peak-on hours. The bi-directional converters are the everlasting key component of an energy storage system due to its ability to condition power from a high-voltage distribution bus (Intermediate 360-400V DC link, or Variable 400-800V DC link, DC Electronic Load) to low-voltage distribution bus (batteries, super-capacitors) and vice versa. The *CLLC* and dual active bridge (DAB) are the two widely adopted DC-DC converter topologies for bi-directional power transfer for an electric vehicle (EV) or an energy storage system (ESS) [1][2][15]. Nonetheless, the soft-switching region for a conventional DAB converter is limited to only narrow output voltage variation [20]. Therefore, the researchers proposed an improved control method for the DAB converter in [17] to improve the conversion efficiency using dual-phase shift (DPS) control. In contrast to DAB, the bi-directional *CLLC* converter can operate with wide output voltage range and soft-switching [2]. Many studies have been carried out over *CLLC* resonant converter. Authors in [2][4] present a design methodology for the *CLLC* converter; these designs make use of wire wound transformer which typically operates at about 50-200 kHz of switching frequency. Nevertheless, none of the aforementioned studies dispense any details on the design and analysis of the high-frequency transformer. To overcome the aforementioned considerations, this paper introduces a detailed design approach and FEA

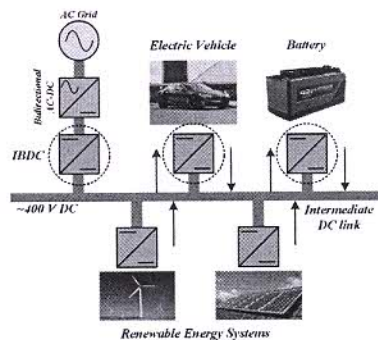


Fig. 1 Typical configuration of LV distribution system using IBDC

backed analysis for the integrated planar transformer. Also, the PI controller is implemented to achieve constant current (CC) and constant voltage (CV) charging of batteries.

The proposed *CLLC* resonant converter for energy storage applications is shown in Fig. 2. The *CLLC* converter has symmetric LLC tank on both primary and secondary sides, resulting in ZVS turn-on of primary side devices and ZCS turn-off of secondary side devices [2][3]. Due to reduced switching loss, the *CLLC* converter is snubber-less [14-17]. The authors in [2][14] present the design methodology and operating modes for *CLLC* resonant converter using fundamental harmonic approximation (FHA). Section II examines the theoretical analysis of the *CLLC* converter, the FHA derived model of *CLLC* converter, forward/reverse modes analysis, and derivations of gain curves. Section III discusses the design methodology for the *CLLC* resonant converter, including the wide input/output voltage range. Section IV presents the design of an integrated planar transformer using PCB stacks for cost optimization. The FEA is performed to estimate the leakage inductance, AC resistance, magnetic flux density, and core losses. Section V presents the hardware experimental results for respective forward and reverse mode of operation; and conversion efficiencies for the same.

## II. THEORETICAL ANALYSIS

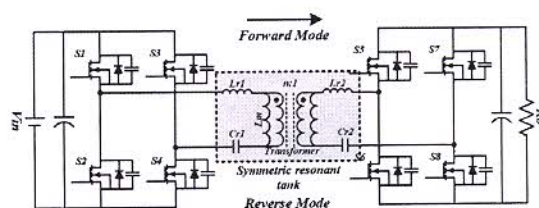


Fig. 2 *CLLC* resonant converter with symmetric LLC tank

Fig. 3 illustrates the waveforms for steady stage operation of the *CLLC* resonant converter operating below the resonant frequency.



### A. Operation of CLLC Resonant Converter

Mode I represent a deadtime duration, during which all switches are turned off and no power is transferred to the secondary rectifying stage. The primary resonant current  $I_{Lr}$ , charges output capacitance of  $S_3, S_4$  and discharges the output capacitance of  $S_1, S_2$ . After this process, the primary current passes through the anti-parallel diode of  $S_1$  and  $S_2$  which makes the switches operate under ZVS.

In II mode  $S_1, S_2$  turns on and power is transferred through the transformer. The  $I_{Lr}$  reverses its direction to positive according to  $S_1, S_2$  because the input source forces the current to positive direction through  $S_1, S_2$ , the output voltage from the secondary is impressed on the magnetizing inductance  $L_m$ , then the magnetizing current  $I_{Lm}$ , builds up linearly. Therefore,  $L_m$  does not participate in the resonance of the primary stage.

In mode III  $I_{Lr}$  equals magnetizing current, at this instant, the power transfer is stopped. Therefore, the secondary current  $I_s$  becomes zero, and the output capacitor is not charged by the output current. The  $I_{Lm}$  will keep rising till  $S_1, S_2$  are turned off. During this mode, the  $L_m$  is no longer clamped by the output voltage. Thus,  $L_r, C_r$  and  $L_m$  participates in resonance together, and the resonant frequency of this mode is slightly different from other modes.

Mode IV is also a deadtime duration with the switch pair  $S_3, S_4$ . The operation is much similar to the mode I; however, the sequence of charging and discharging switches pair is

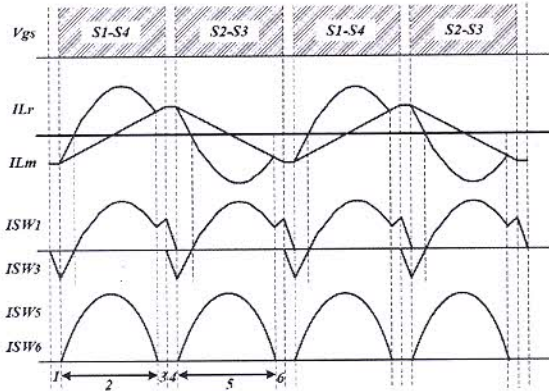


Fig. 3 Operating modes of the CLLC resonant converter at below resonance

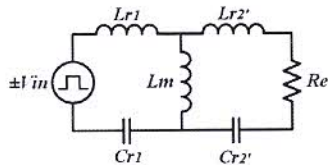


Fig. 4 Equivalent circuit of CLLC converter in battery charging mode (BCM)

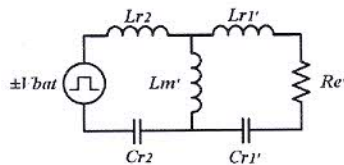


Fig. 5 Equivalent circuit of CLLC converter in reverse mode (RM)

different. The  $I_{Lr}$  discharges the output capacitances of  $S_3, S_4$  and charges the output capacitances of  $S_1, S_2$ ; and  $S_4, S_5$  can turn on with ZVS.

In mode V  $S_3, S_4$  turn on and starts transferring power to the secondary side. During this mode, the  $I_{Lr}$  changes direction due to the impressed voltage but now in the opposite direction to that in mode II.

After the execution of Mode 5, the resonance and power transfer stops. With no power, the  $I_s$  becomes zero and the anti-parallel diodes of output rectifier are softly commutated. A similar operation occurs in the reverse mode, only load, and supply voltage changes.

### B. Gain Analysis of CLLC Resonant Converter

#### i. Equivalent Circuit in the Forward Mode (BCM)

The equivalent circuit of the CLLC converter in the forward mode is shown in Fig. 4. Assuming that 'n' is the transformer's turns ratio. Using the FHA, equivalent load resistance  $R_e$  can be expressed as follows [2][5].

$$R_e = \frac{8n^2}{\pi^2} R_o \quad (1)$$

Where,  $R_o$  is the load resistance in the forward mode. All the equivalent resonant parameters referred to the primary side are as follows.

$$L'_{r2} = n^2 L_{r2}, C'_{r2} = \frac{C_{r2}}{n^2}, \quad (2)$$

The normalized frequency, quality factor, and the resonant frequency is defined as (3)

$$\omega = \frac{\omega_s}{\omega_r}, Q_f = \frac{\sqrt{L_{r1}}}{R_e}, \omega_r = \frac{1}{\sqrt{L_{r1} C_{r1}}} \quad (3)$$

#### ii. Equivalent Circuit in the Reverse Mode (RM)

The Equivalent circuit of the CLLC converter in reverse mode is shown in Fig. 5, similar to (1) the equivalent load resistance ( $R_e'$ ) can be calculated using FHA [2][5][13-14] and is shown in (4)

$$R_e' = \frac{8}{n^2 \pi^2} R'_o \quad (4)$$

Where,  $R'_o$  is the load resistance in reverse mode. Similarly, all the resonant parameters referred to the secondary are as follows.

$$L'_{r1} = \frac{L_{r1}}{n^2}, C_{r1} = n^2 C_{r1}, \omega_r = \frac{1}{\sqrt{L_{r2} C_{r2}}} \quad (5)$$

$$Q_r = \sqrt{\frac{L_{r2}}{C_{r2}}}, L'_m = \frac{L_m}{n^2}$$

#### iii. Gain Curves for Forward and Reverse Modes

The general transfer function  $H(s)$  can be derived by analyzing Fig. 4 and is expressed in (6)

$$H(s) = \frac{nV_{out}}{V_{in}} = \frac{R_e(R_2 // sL_m)}{R_2(sL_{r1} + \frac{1}{sC_{r1}} + R_2 sL_m)} = \frac{V_{in}}{(\frac{1}{sC_{r1}} + sL_{r1}) + (n^2 sL_{r2} + \frac{n^2}{sC_{r2}} + \frac{8n^2}{\pi^2} R_o) [1 + \frac{1}{sL_m} (\frac{1}{sC_{r1}} + sL_{r1})]} \quad (6)$$

Where,

$$R_2 = R_e + sn^2 L_{r2} + \frac{n^2}{sC_{r2}} \quad (7)$$

The gain function of CLLC converter in the forward mode is derived in [5], which is expressed as (8)

$$|H(s)|_f = \frac{nV_{out}}{V_{in}} = \frac{1}{\sqrt{((\frac{1}{h} - \frac{1}{h\omega^2} + 1)^2 + [\frac{1}{\omega}(\frac{m}{h} + \frac{1}{hg} + \frac{1}{g} + 1)]Q_f - \omega(\frac{m}{h} + m + 1)Q_f - \frac{Q_f}{hg\omega^3})^2}} \quad (8)$$

Where,



$$h = \frac{L_m}{L_{r1}}, m = \frac{n^2 L_{r2}}{L_{r1}}, g = \frac{C_{r2}}{n^2 C_{r1}}$$

Similarly, the gain function for reverse mode can be expressed as in (9)

$$|H(s)|_r = \frac{1}{\sqrt{\left(\left(\frac{1}{p} - \frac{1}{p\omega^2} + 1\right)^2 + \left[\frac{1}{\omega} \left(\frac{r}{p} + \frac{1}{pq} + \frac{1}{q} + 1\right) Q_r - \omega \left(\frac{r}{p} + r + 1\right) Q_r - \frac{Q_r}{pq\omega^3}\right]^2\right)}} \quad (9)$$

Where,

$$p = \frac{L_m}{n^2 L_{r2}}, r = \frac{L_{r1}}{n^2 L_{r2}}, q = \frac{n^2 C_{r1}}{C_{r2}}$$

### III. DESIGN METHODOLOGY

The resonant frequency  $F_r$  is selected 300-350 kHz for forward and reverse modes considering the trade-offs between EMI, power density, and efficiency. [12] presents a shielding technique to suppress the common-mode (CM) EMI for an LLC resonant converter employing the planar matrix transformer. Reducing the resonant frequency can help in the reduction of core and copper losses in the transformer but, may cause severe EMI issues [11]. The input voltage range is selected as 360-400V; the converter is aimed to charge low voltage batteries (40-60V) for battery-based energy storage systems; in this view, the turns ratio of transformer  $T_r$  is chosen to 7.5. The gain of the converter can be calculated as per the following equation:

$$\frac{V_{out}}{V_{in}} = \frac{G_{forward}}{n} \quad (10)$$

Fig. 6 shows the gain curves for both forward and reverse modes.

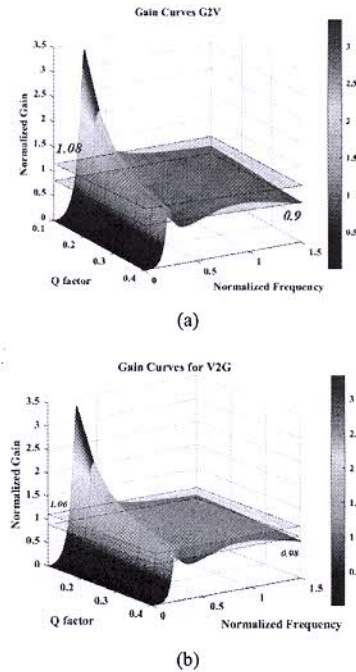


Fig. 6 Gain characteristics of the CLLC resonant converter in forward (BCM) and reverse (RM) mode

#### A. Design of Magnetization Inductance to attain Soft-Switching

ZVS turn-on for high voltage devices and ZCS turn-off for low voltage devices are pivotal to achieve optimal conversion

efficiency. The  $L_m$  should be designed such as the turn-off current discharges the devices capacitances ( $C_{oss}$ ) within deadtime to achieve soft or ZVS turn-on. In adjunct, operating below the resonant frequency can guarantee the soft commutation of the low voltage devices, because it effectively increases the deadtime duration [2][10][14]. Therefore, the  $L_m$  is limited by the maximum switching frequency and is given by (10)

$$L_m \leq \frac{T_{dead}}{16 C_{oss} F_{rmax}} \quad (11)$$

Where,  $F_{rmax}$  is the maximum operating frequency,  $T_{dead}$  is deadtime; a small  $L_m$  guarantees ZVS of high voltage devices at the primary side but small  $L_m$  can increase the turn-off losses, and larger  $L_m$  causes loss of ZVS; anyhow, both abbreviate the conversion efficiency [2].

#### B. Resonant Tank Design

Resonant elements must be designed for every possible operating point viz. load changes, frequency changes, circulating energy, and input/output voltage variations [2][10]. The nominal input voltage is kept at 360 V and the nominal load is 4.2  $\Omega$  in the forward mode (BCM) and 330  $\Omega$  in reverse mode (RM). The turns ratio of the transformer is selected as 7.5:1 considering the 360 V nominal input and 50 V output. The  $Q$  factor of the resonant tank is selected as 0.18 ( $Q_1$ ) for the forward mode and 0.15 ( $Q_2$ ) for reverse mode, delivering 500W of output power. The resonant tanks elements are selected as per the following:

$$C_r = \frac{1}{2\pi Q_1 F_r R_e} \quad (12)$$

$$L_r = \frac{1}{C_r 2\pi F_r^2} \quad (13)$$

$$L_m = L_n L_r \quad (14)$$

To reduce the size and weight of the passive elements, the transformer's leakage inductance is utilized as resonant inductors for both sides, which eliminates the additional losses which would have been incurred due to external inductors.

Table IV enlists the key designed parameters for the CLLC resonant converter.

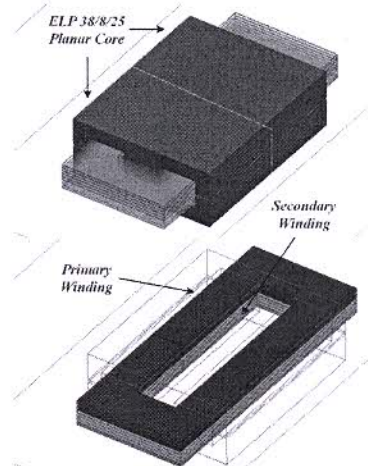


Fig. 7 Construction of the proposed integrated transformer employing two ELP38/8/25 cores and PCB stack windings

